Piezoelectric charging and wireless communication

Hyeong Jae Lee, Xiaoqi Bao, Stewart Sherrit, Yoseph Bar-Cohen, Mircea Badescu, and Shannon Jackson
Jet Propulsion Laboratory, California Institute of Technology, 4800 Oak Grove Drive, Pasadena, CA, USA 91011

© 2018. California Institute of Technology. Government sponsorship acknowledged.

ABSTRACT

Modern medicine is undergoing a revolution in the application of new sensor capabilities for aiding in diagnosis of specific conditions and monitoring a variety of informative vital signs. In the past, many of the measurements were limited by what could be accomplished externally. A shift toward in-vivo monitoring for both diagnostic and therapeutic sensing and actuation [1] has created a need for low power electronics, high energy density batteries and methods to successfully power devices embedded in the body. For a review of the field and sensing capabilities see [2]. Recent studies suggest that charging with ultrasound is more efficient at longer transmission distance (> 10cm) than inductive charging [3]. In this manuscript, we discuss the modeling and experimentation that we have accomplished and demonstrate in ultrasonic charging of sensors having the form and fit of in-vivo sensors. The task goal has been to use piezoelectric transducers for wireless communication and powering of sensors internal to the human body with a goal to transmit power levels of 100 μW a receiver with receiving area of 3x3 mm^2 over a distance of 16 cm equivalent to human body interior. The results suggest that we can transmit power levels that exceed this baseline requirement.

Keywords: Piezoelectric, remote-charging, wireless, composites, transducer

1. INTRODUCTION

The system investigated in this manuscript is shown schematically in Error! Reference source not found.. The working principle of ultrasonic wireless power delivery has been described previously [4-7]. Briefly, an ultrasonic transducer external to the body produces an ultrasonic wave that travels through the body tissues to an embedded ultrasonic transducer and the pressure wave generates electricity at the embedded transducer. The electricity is conditioned to supply power to a storage unit (battery) or an in-vivo sensor directly. The sensor information is then transmitted using the receiving transducer and the information is transmitted to an external ultrasonic transducer where it is recorded and decoded. Alternatively, the receiving transducer could power a wirless Electro-Magnetic (E/M) transmitter and transmit the data back to a wireless base station. The investigated system has the ability to transmit power to internal sensors and receive data from them.

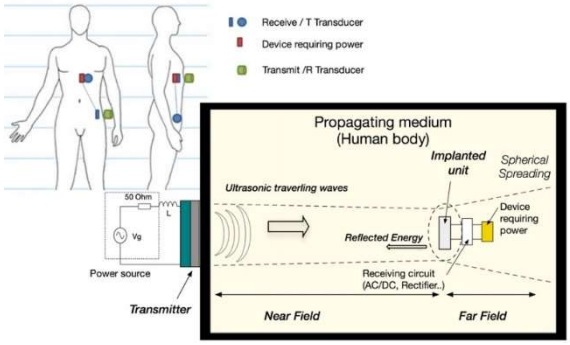

Figure 1. Ultrasonic system for wireless power delivery

In this research and development task, we sought to use piezoelectric transducers for wireless communication and powering of sensors internal to the human body to distances of 16 cm and at power levels of 100 µW or greater. The volume footprint of the internal sensor was of the order of 3mm x 3mm x 1 mm mm while the volume and size of the external transducer was kept to below 3.75 cm (1.5") in diameter. In addition, previous studies on the safe intensity of ultrasound for the human body found that 100 mW/cm^2 level or (38,730 Pascals) has been most extensively studied and has never shown to produce a biological effect [8]. We designed the transducers which are suitable for ultrasonic wireless power transmission/reception system based on design theory led by both network models [9] and finite element modeling. The performance was experimentally investigated and the results were compared to the modeling results.

2. THEORETICAL BACKGROUND

Mason and KLM models are two well known one dimensional models for modeling of an ultrasonic transducer, which is based on equivalent network models of transducers. In this manuscript, the KLM model was used to model an ultrasonic transducer for wireless power delivery [10-12] and this section gives a brief summary of the information needed to implement the KLM model using a transfer matrix approach and points out the critical features for accurate power transfer modeling. The KLM network representation of an ultrasound transducer is shown in **Figure 2**. The electro-mechanical conversion is modelled as a perfect transformer with a winding ratio Φ :1. Matching and backing layers can be easily added using their thickness and acoustic impedance values represented as an acoustic transmission line. The definitions of circuit components are given below:

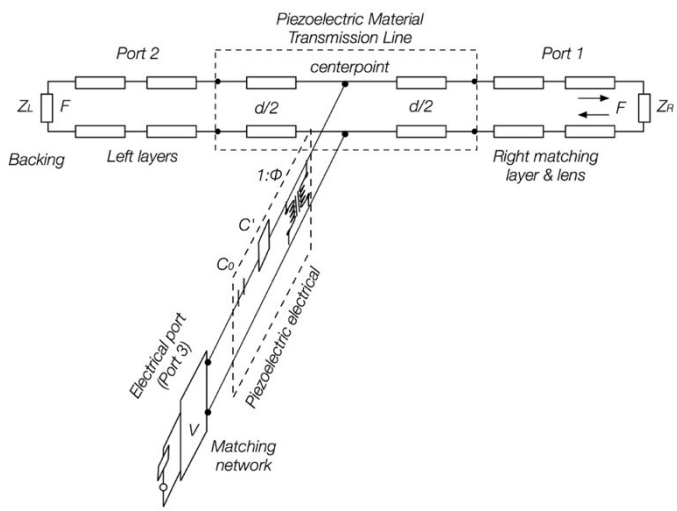

Figure 2. KLM model for a piezoelectric transducer producing a pressure field. Voltage is applied on the electrical port and pressure is developed across the front acoustic port. Pressure wave is received by the transducer and it produces electricity in the load resistor.

$$C_0 = \frac{\varepsilon_0 \varepsilon_r A}{t}$$
$$C_0' = \frac{C_0}{k_t^2 \operatorname{sinc}\left[\frac{\omega}{\omega_a}\right]} \tag{1}$$
$$\Phi = k_t \sqrt{\frac{\pi}{\omega_a C_0 Z_C}} \operatorname{sinc}\left[\frac{\omega}{2\omega_a}\right]$$

where ε_0 and ε_r are the dielectric permittivity in vacuum and medium respectively, and A is cross-sectional area of the piezoelectric layer. k_t, ω_a, and Z_C, are the electromechanical coupling factor, antiresonance angular frequency, and the

acoustic impedance of the transducer element, respectively. The mechanical delay line of piezoelectric transducer and/or matching layer is represented by Eq. (2).

$$\begin{pmatrix} \cosh[k.l] & -Z_l \sinh[k.l] \\ -\sinh[k.l]/Z_l & \cosh[k.l] \end{pmatrix} \tag{2}$$

where Z_l, k and l are the acoustic impedance, complex propagation constant (k=α+jβ, β=2π/λ and α is attenuation) and the thickness for piezoelectric and the matching layers, respectively. For wireless power transfer, it is critical to consider the intrinsic loss in the material. Losses in the piezoelectric material consist of the mechanical losses (Q_m^{-1}) due to damping of mechanical vibrations and electrical losses associated with polarization lag or leakage current and modeled using the imaginary part of the capacitance of the element (tan δ). The mechanical impedance for each layer and the capacitance of piezoelectric material are, thus, described by following complex numbers:

$$\begin{aligned} Z' &= Z(1-\frac{j}{2Q_m}) \\ C_0 &= C_0(1-jtan\delta) \end{aligned} \tag{3}$$

To calculated transmit power efficiency of ultrasonic transducers, we first obtained the transmit and receive transfer functions using a transfer matrix approach. The relationships between the circuit quantities and a transfer matrix (ABCD) of the piezolectric are given by:

$$\begin{pmatrix} F_R \\ u_R \end{pmatrix} = \begin{pmatrix} A & B \\ C & D \end{pmatrix} \cdot \begin{pmatrix} V_g \\ I_g \end{pmatrix} \tag{4}$$

where V_g and I_g are the source voltage and current, respectively, and F_R and u_R are the mechanical force and particle velocity, respectively. The overall transfer ABCD-matrix coefficients for piezoelectric transducer are then obtained by the product of the individual matrices corresponding to the electrical matrix, electro-mechanical matrix, the piezoelectric element, and the matching layers (**Figure 3**).

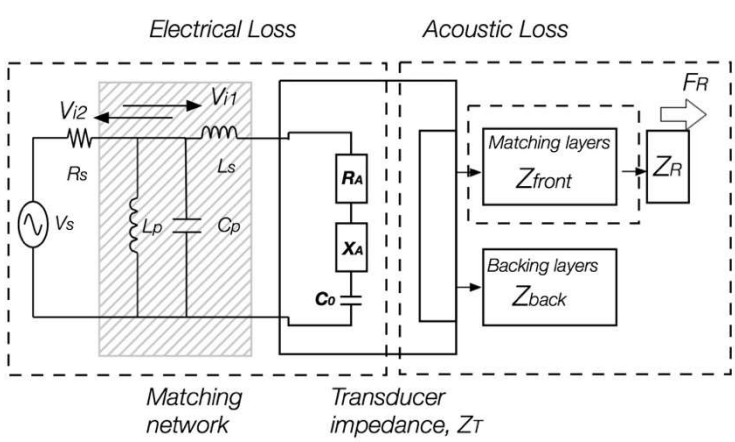

Figure 3. A schematic drawing of a transmitter system.

The boundary conditions of the parameters listed in Eq. (4) are

$$
\begin{aligned}
V_g &= V_{i1} + V_{i2} \\
I_g &= (V_{i1} - V_{i2}) / Z_T \\
u_R &= F_R / Z_R
\end{aligned}
\tag{5}
$$

where the subscript i1 and i2 indicate a plane wave in the positive and negative direction, respectively. Z_R and Z_T are the radiation impedance and electrical impedance of the transducer, respectively. Then, the transmit transfer function and electrical impedance of the transducer can be obtained by substituting Eq. (5) into Eq. (4):

$$
\begin{aligned}
tf(\omega) &= \frac{F_R}{V_T} = \frac{2Z_R}{B - Z_T A - Z_R D + Z_T Z_R C} \\
Z_T &= \frac{A_t Z_R + B_t}{C_t Z_R + D_t},
\end{aligned}
\tag{6}
$$

where A_t, B_t, C_t and D_t are matrix coefficients resulting from the inverse of the matrix defining the parameters for the transmit ABCD network.

The electrical energy losses, defined as the power reaching the transducer divided by the maximum power available from the source, is given by:

$$
EL = \frac{P_E}{P_G} = \frac{I_T^2 R_T / 2}{V_g^2 / 8R_g} = \left|\frac{V_T}{V_g}\right|^2 \frac{4R_T R_g}{|Z_T|^2}
\tag{7}
$$

where

$$
\frac{V_T}{V_g} = \frac{Z_T}{Z_T + Z_s + R_g}
\tag{8}
$$

Combining the Eqs. (7) and (8),

$$
EL = \frac{4R_T R_g}{(Z_T + Z_s + R_g)^2}
\tag{9}
$$

The acoustic loss, defined as the ratio of the radiated acoustic power P_R, to the power of the excitation electrical power delivered into the transducer P_E, can be calculated as follows:

$$
AL = \frac{P_R}{P_E} = \frac{F_R^2 / (2Z_R)}{I_T^2 R_T / 2} = \left(\frac{F_R}{V_T}\right)^2 \frac{Z_T^2}{Z_R R_T} = tf(\omega)^2 \frac{Z_T^2}{Z_R R_T}
\tag{10}
$$

The total transducer losses (power efficiency) from the transmitter can be written as the product of electrical loss and acoustic loss.

$$\eta_T = \frac{P_R}{P_G} = EL \times AL \tag{11}$$

The reception system is the reciprocal of the transmitting system, so it can be modeled as a two port system which converts the acoustic waves at the mechanical port to the electrical energy at the electrical port (see **Figure 4**).

$$\begin{pmatrix} V_R \\ I_R \end{pmatrix} = \begin{pmatrix} A_t & B_t \\ C_t & D_t \end{pmatrix} \cdot \begin{pmatrix} F_T \\ v_T \end{pmatrix} \tag{12}$$

where V_R and I_R are the voltage and current at the electrical port, respectively, and F_t and v_t are the total force acting on the face of the transducer and the velocity of the transducer surface respectively. In the reception system, the acoustic waves incident on the transducer face are reflected back. These incident and reflected waves create a force on the transducer face and excite the piezo crystal, thus, $F_T = F_i + F_s = F_i - Z_R v_T$.

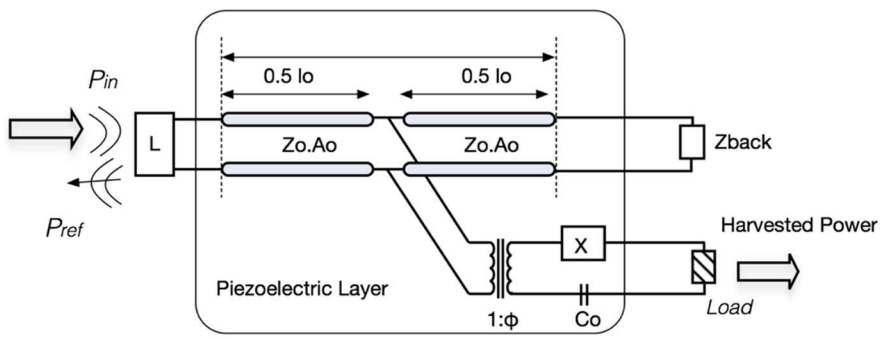

Figure 4. A schematic drawing of a reception system.

According to the Eq. (12), the receiving transfer function can be obtained as follows:

$$tr(\omega) = \frac{V_{OC}}{F_i} = \frac{2Z_T}{B_t + Z_T D_t + Z_R A_t + Z_T Z_R C_t} \tag{13}$$

For the electric power generation, when the external resistive load (R_L) is connected to the piezoelectric harvester, the voltage and the average power delivered to the resistive load, assuming that the piezoelectric material is an ideal capacitor and the dielectric loss of the piezoelectric structure is infinitely small, are given by,

$$\begin{aligned} V_L &= V_{OC} \left| \frac{R_L}{Z_T + R_L} \right| \\ P_L &= \frac{V_L^2}{2R_L} \end{aligned} \tag{14}$$

where R_L and Z_T are the load resistance and the transducer impedance, respectively. The total power received on the transducer face, P_T is given by:

$$P_i = \frac{F_T^2}{2Z_R} \tag{15}$$

Note that the effects of wave diffraction and scattering effects are very important but are not considered here. Assuming that there are no wave diffraction effects at the edges of the receiving transducer [11, 13], the power ratio of harvesting power (P_L) and received power on the transducer faface (P_T) is then obtained by combining Eqs. (13), (14) and (15):

$$\eta_R = \frac{P_L}{P_T} \approx 4\left(\frac{tr(\omega)}{R_L + Z_T}\right)^2 Z_R R_L \tag{16}$$

3. MODELING RESULTS

Initially we applied KLM model to three different receiving transducer designs. The parameters of the designs are shown in **Table 1**. The receive sensitivity for the three transducer designs is shown in **Figure 5**, where the green thick line shows an open circuit on the electrical port. The colored thin lines from low to high are the sensitivity with different resistance loads starting from 237.3 Ohm and increasing to 9729 Ohm in steps of 949.2 Ohm.

Table 1. The piezoelectric parameters of three transducer designs

1-3 composite (35% P5H):							
	k_t	ε_s	A (cm^2)	C_0 (pF)	Q_m		
PZT:	0.67	592	0.0707	25.56	30		
Layers	Velocity	Density	Impedance	Thickness	Thickness in Wavelength	Attenuation	Resonance
	m/s	kg/m^3	MR	mm		dB/cm	MHz
PZT Disk:	3620	3323	12.03	1.45	0.5	3.14	1.2491
Matching:							
Backing:			0				
Front:			1.5				
P5A and matching layer							
	k_t	ε_s	A (cm^2)	C_0 (pF)	Q_m		
PZT:	0.49	830	0.0707	25.12	70		
Layers	Velocity	Density	Impedance	Thickness	Thickness in Wavelength	Attenuation	Resonance
	m/s	kg/m^3	MR	mm		dB/cm	MHz
PZT Disk:	4600	7500	34.5	2.07	0.5	0.94	1.1125
Matching:	3053	2359	7.19	0.69	0.25	5	
Backing:			0				
Front:			1.5				

The received electric power is a function of frequency and the resistive load. The maximum power was calculated for each resistive load. we obtained sensitivity and the reflection coefficient were combined along with a limiting pressure amplitude of 38.73 kPa on a 3 mm diameter disk transducer to determine the output voltage and the power delivered as a function of the electrical load. The results and the corresponding voltage are shown in **Figure 6** where the incident wave intensity is set as 100 mW/cm ^{2} (or 38,73 kPa) and the receiving area of the transducer is a disk of 3 mm in diameter. The received power over a broad load impedance range for all the three transducer designs are above 4 mW which suggests that the target of 0.1 mW is feasible for transducers having 3 mm diameter. The composite and the PZT 5A with matching layer could produce about 5.2 mW power. The results show better performance for the composite and the transducer with matching layer.

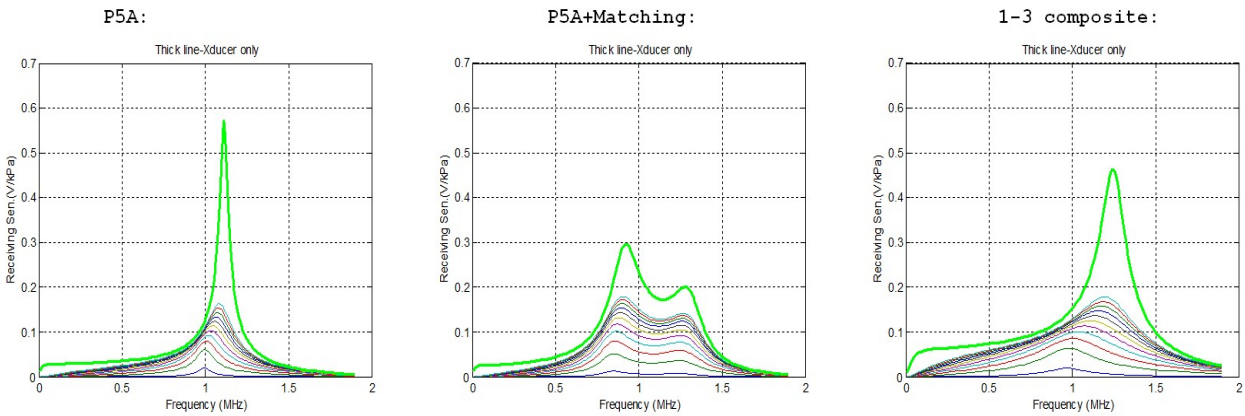

Figure 5. The transducer receive sensitivity for a bare piezoelectric disk (P5A), a piezoelectric disk with a matching layer (P5A + Matching) and for a 1-3 composite transducer as a function of frequency and for different impedance on the electrical port.

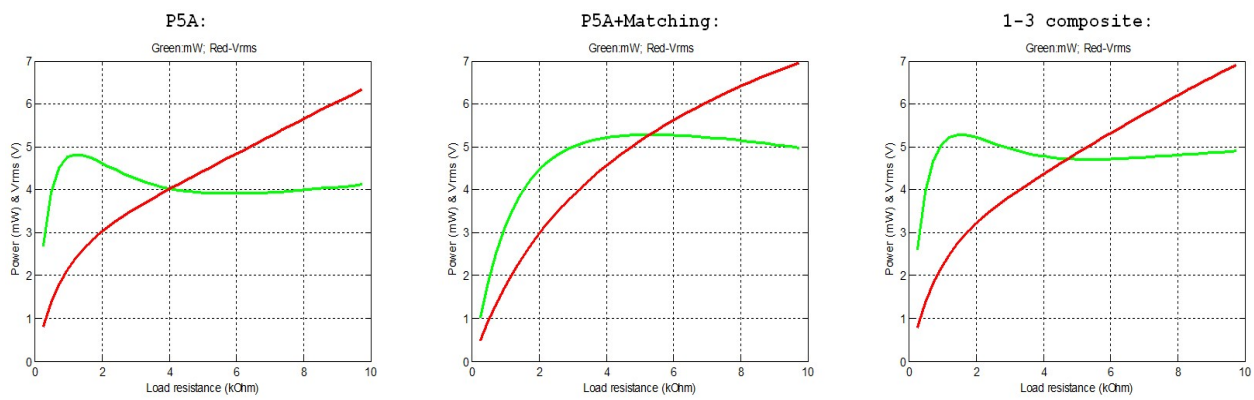

Figure 6. Power levels and generated voltage as a function of the electrical load resistance. The 1-3 composite and the PZT 5A with Matching layer show better performance

The modeling analysis above suggests that obtaining power levels at an imbedded transducer of the order of 100 μW is feasible, however this analysis was based on the pressure levels impinging on the transducer were 38.73 kPa. In reality, there are varieties of loss mechanisms that can reduce the pressure at the transducer surface. The first aspect of the transducer is the transition between the near and far field of the ultrasonic signal. Ideally, one wants to stay in the near field. The length of the near field region is governed by the diameter of the transducer and the wavelength of the ultrasound. In the simplest case of a piston transducer the near field is found to extend to $L = D^2/4\lambda$ after which the far field develops and the pressure decreases linear with the divergence angle $\sin\theta = v/Df$, where v is the acoustic velocity, D is the transducer diameter and f is the frequency. It should be noted that receiver transducers of 5mm diameter or smaller have a large enough directivity angle to tolerate a positioning change of up to 20 degrees at frequency of 1 MHz.

In addition to the location of the receive transducer in the ultrasonic field and the beam divergence, one also has to consider the attenuation in the human body. A general attenuation coefficient associated with tissue absorption is about 0.75 dB/cm/MHz. The estimate as a function of frequency of the total attenuation in dB due to the transmission of the ultrasound in 16 cm of tissue was done for four different transducer diameters by using a simplified model. At a given frequency and transducer diameter, the length of the near field was calculated and if the length exceeded the 16 cm, only the tissue absorption attenuation was applied. If the near field length was short of the 16 cm transmission length the attenuation due to the increase of the beam area by divergence was added

The attenuation results are shown in **Figure 7** for the 4 different diameters of transmitters as a function of frequency. A 20 dB change is a reduction of 10 times in the pressure and 100 times the power. Based on the 5 mW power generation for the transducers with no transmission loss, we see that a total attenuation of 17 dB would reduce the power levels to the 100 μW. The data in **Figure 7** suggest that, operating at a frequency of 1.25MHz or lower, we could use the 1"or larger

transmitters to achieve the goal of obtaining more than 100 μW by the receiver at 16 cm distance while the initial transmission intensity is not over the limit of 100 mW/cm ^{2} . The transmission performance could be improved if a focused transmitter is applied.

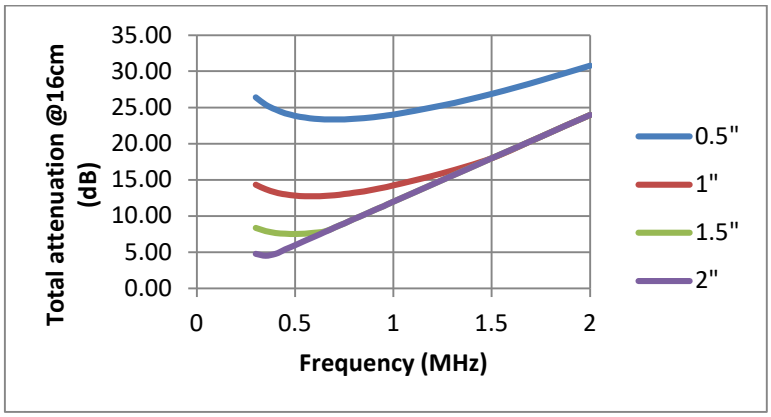

Figure 7. The total attenuation including divergence and tissue absorption loss for 4 different transducer diameters as a function of frequency.

4. DESIGN AND CHARACTERIZATION OF 1 MHZ TRANSMITTER AND COMPOSITE BASED RECEIVER

4.1 Transmitter design

In order to produce an efficient ultrasonic wireless power transmission and reception, high transmitting or receiving sensitivity are needed. This can be achieved with coupled resonant type transducer system due to its increased output power and/or higher receiving sensitivity at the resonant frequency. In order to improve the transfer of energy from/to the transducer, quarter-wave matching layers are used. These can be produced by manufacturing an acoustic impedance equal to the geometrical mean value of the impedances of transducer material and radiation medium at a thickness of a quarter wavelength bonded at the front surface of a transducer. However, such conditions are generally suitable for non-resonant applications that require broad bandwidth to produce sharp pulses. An example of this case is in medical imaging applications. These transducers generally use a highly attenuating backing material so that the backward travelling waves are not reflected back into the piezoelectric layer, and the backing material broadens the transducer response decreasing the resonance response. In the case of resonant type transducer, although the quarter-wave matching layer can improve power transmission, it results in damping in the piezoelectric material, reducing both transmitting or receiving sensitivity at resonance however it produces a larger frequency region to excite the transducer.

Figure 8 shows the simulated transmit sensitivity, transducer loss and transmit power efficiency of epoxy backed transmitter. The power transmission efficiency of the system (η_T) is determined as the ratio between the radiated acoustic power and the input electrical power, (see Eq. (15)). The comparison between the measured and the simulated transmit sensitivity was used to validate the model. For the measurement of acoustic output power from the transmitter, a radiation force method was used to calibrate the acoustic power. The force is measured with a right-angled conical reflecting target (Ohmic Instruments UPM-DT-10 power balance), which can measure up to 30 watts with a display resolution of 20 milliwatts. The transducer was facing down and positioned above the metal cone reflector in distilled water. The input voltage of function generator was adjusted to have the same input voltage over the frequency range of interest (800 kHz - 1 MHz), and the corresponding output powers were measured. From the plot, it was found that the implemented model showed good agreement with the measurement results. The transmit sensitivity is about 4.5 kPa/V over the range of 0.8 MHz to 1 MHz with transmit efficiency $>$ 25%.

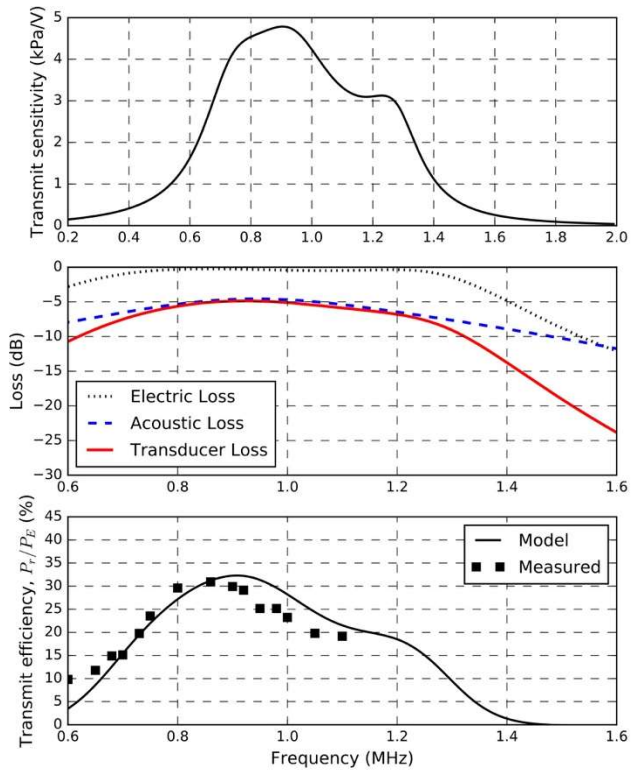

Figure 8. Simulated transmit sensitivity, transducer loss and transmit efficiency of the epoxy backed transmitter with matching layer. Measured transmit efficiency is plotted for comparison.

4.2 Composite based receiver

In the design of resonant type receivers, it is critical to consider spurious mode coupling with the desired thickness mode vibration since mode coupling reduces the transmitting/receiving energy and consequently reduces transducer performance. The half-wave lateral mode of the elements should be well above or below the fundamental thickness vibration so that their harmonics do not couple to the thickness mode. A high width-to-thickness aspect ratio (> 10) of piezoelectric elements are generally preferred for pure thickness mode vibration. For the purpose of bio-implantable devices, the size of receiver should be millimeter-scale, no higher than 5 mm of width or diameter, and for 1 MHz operating frequency, the required thickness is around 2 mm, making it difficulty to develop pure resonant type transducers without mode coupling issues with conventional piezoelectric materials.

Piezoelectric/polymer composites with 1-3 connectivity, specifically the random fiber composites, provide an effective solution as the random structure (placement of the fibers) will be able to suppress the lateral modes in the composite, mitigating interference of fundamental thickness vibration from these wave vibrations. Additional advantage of piezocomposites over monolithic piezoelectric ceramics is low acoustic impedance. Although piezoelectric ceramics, such as PZT, offer high electromechanical properties, they suffer from high acoustic impedance (around 35 MRayl) as a result from high density of PZT ceramics, which impede the energy flow between the transducer and tissue (1.5 MRayl) [14]. For this study, we used low volume percent (35 %) of 1-3 piezo composites from Smart Materials Corp. (http://www.smart-material.com). Bulk properties of the composite, summarized in **Table 2**, were measured and used in the KLM equivalent circuit model.

Table 2. Material properties and geometric parameters of the composites used for KLM model.

Vol (%)	w/l/t (mm)	ρ (kg/m^3)	v_l (m/s)	$\varepsilon_{33}^T/\varepsilon_0$	$tan\delta$
35	5/5/1.5	3467	3489	1386	0.018

f_r (MHz)	f_a (MHz)	k_t	Q_m	$\varepsilon_{33}^{S}/\varepsilon_0$	Z (MRayl)
1	1.151	0.52	60	700	12

Using KLM transmission line model, power receiving efficiency of the composite receiver (P_L/P_T) as a function of the load resistance and excitation frequency were calculated and the results are plotted in **Figure 9**. The results show that the maximum receiving power efficiency over 90 % can be achieved around the resonant and anti-resonant frequency of the composte based receiver.

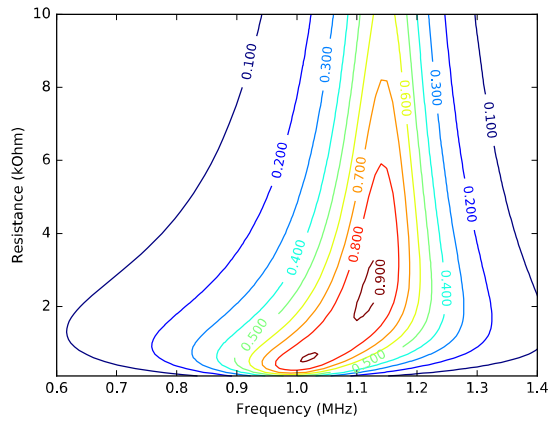

Figure 9. Contour plot of receiving power efficiency (power output normalized with respect to the input power) versus the excitation frequency and load resistance.

Several composite based receivers without quarterwave matching layers were fabricated, where the thickness of front layer is around 2 mm, and its acoustic impedance is 3 MRayl. The spectra of the in-air electrical impedance and phase of the fabricated composite transducers are shown in **Figure 10**. For comparison, in-air impedance and phase spectra of the 1-3 composite materials under a free vibration condition are plotted in the figure. It is observed that the fabricated composite based receivers show a reduction of the resonance frequencies and electromechanical coupling factor, compared to the as-received 1-3 composites. This is likely due to the acoustic radiation impedance from the added components during receiver fabrication, such as the front layer, soldering the wires on the back, which can damp and shift down the resonsonce of the composite receiver. It should be noted that the reactance of composite based receivers is not equal to zero at resonance which drops the voltage developed across the resistor due to charging the complex component. For the maximum power extraction, the electrical impedance matching can be done using a series inductor ($L_s=1/(\omega^2 C_o)$), which tune out the value of remaining reactance at resonant frequency.

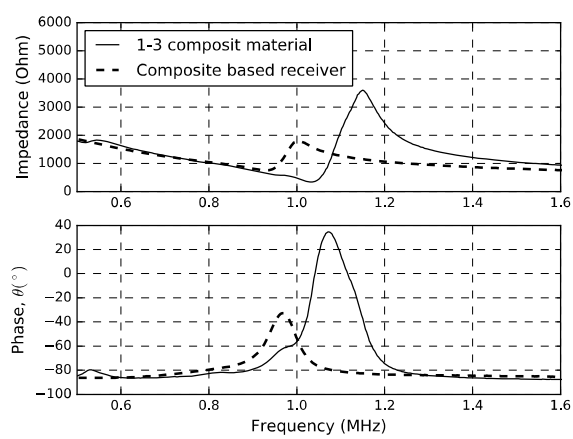

Figure 10. Measured electrical impedance and phase spectra of air-backed 1-3 composite receiver.

Figure 11 shows the electrical impedance and phase of tuned composite based receivers measured in water. After tuning, the inductor removes capacitive reactance, X from the electrical system; thus, the phase angle becomes zero and the transducer electrical impedance was reduced to around 100 Ohm in the frequency range of interest.

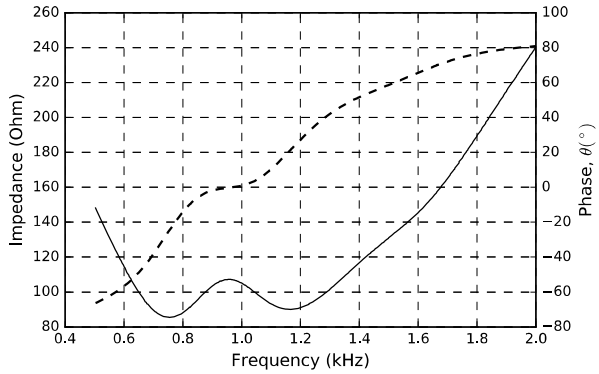

Figure 11. Electrical impedance (solid line) and phase (dashed line) spectra of air-backed 1-3 composite transducers after tuning.

For the measurement of harvesting electrical power from the receivers, the receivers were placed >20 cm from the transmitter surface inside water tank (**Figure 12**). The open circuit voltage signals from the piezoelectric receivers were measured by transmitting 100 mW/cm^2 output power density over the frequency range of the test to determine optimum receiving frequency. **Figure 13** shows the obtained results exhibiting receiving sensitivity (μV/Pa) of composite based receivers as a function of frequency. Note that the maximum sensitivity was achieved around 0.95 -1 MHz, exhibiting 140-150 uV/Pa.

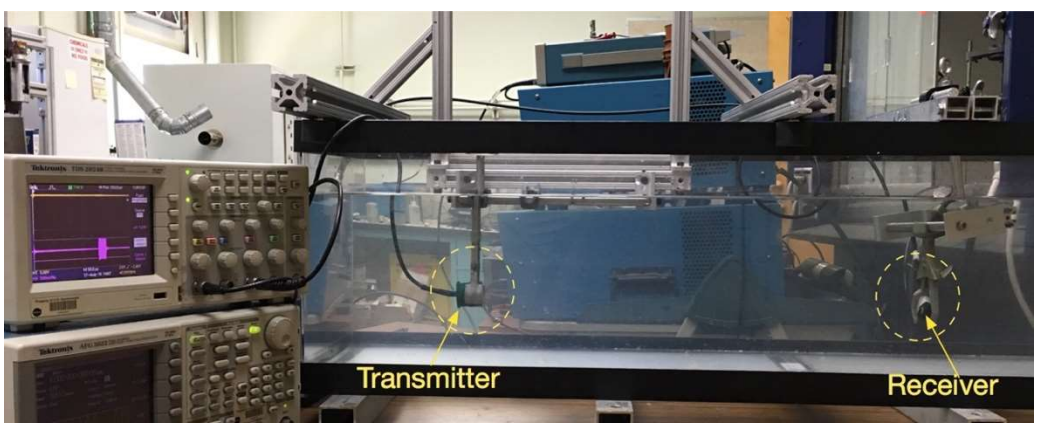

Figure 12. Experimental setup for acoustic test tank with positioning system.

The power output generated by the composite receivers as a function of the load resistance is shown in **Figure 14** at the 100 mW/cm^2 of acoustic power with 1 MHz frequency. The maximum power levels of the composite transducers under 100 mW/cm^2 of transmit power were found to be 23 mW (or 92 mW/cm^2), exhibiting $>90\%$ of the receiving efficiency. Considering the attenuation of typical human tissue (0.75 dB/cm/MHz), the received power level at 16 cm distance in human tissue would be 1.45 mW on 5x5mm receiving area or 522 μW on 3x3mm after 12 dB power loss, which is still significantly higher than 100 μW of the project goal.

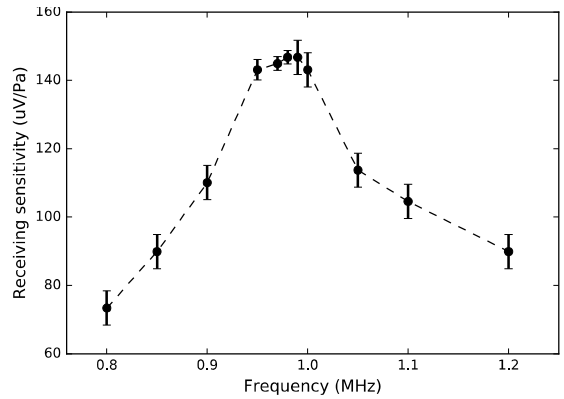

Figure 13. Receiving sensitivity (open circuit voltage / pressure) of composite transducers at 1 MHz as a function of frequency under an input watt density of 100 mW/cm^2.

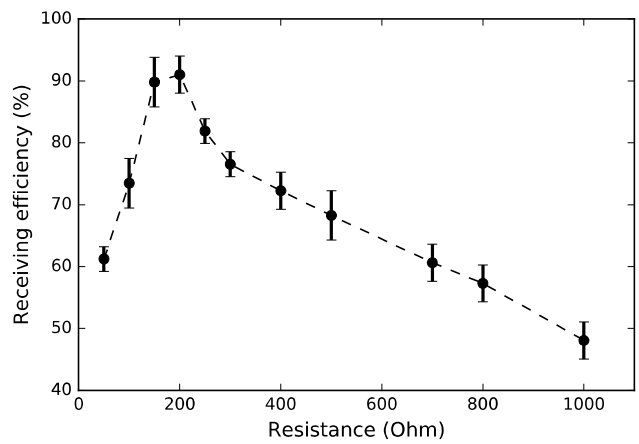

Figure 14. Transferred power efficiency of the composite based receiver as a function of load resistance.

5. CONCLUSION

Ultrasonic power offers an excellent alternative to charging implantable medical devices where the location and the size restrict the usage of a battery or inductive powering. Ultrasonic waves can propagate through the body with relatively little attenuation, allowing one to transmit power at larger distances. Analysis was undertaken to determine the optimum transducer design for powering imbeded sensors for In-vivo sensing. The electrical, acoustic and attenuation were accounted for in the models as well as the location in the near field. The models suggest that a charging system with power levels above 100 μW can be produced after all the loss mechanisms were accounted for. A variety of transducer transmitter and reciever pairs were manufactured and tested based on the results of the 1D and FEM models. The 1-3 composite based receivers were able to convert >90 % of incident wave power on receiving surface at the matched load at 20 cm away, proving their suitability for the bio-implanted device. The calculated power level at 16 cm distance in human tissue (using an attenuation of 0.75 dB/cm/MHz) would be 1.45 mW on 5x5 mm^2 after 12 dB power loss was accounted for.

ACKNOWLEDGEMENTS

Research reported in this manuscript was conducted at the Jet Propulsion Laboratory (JPL), California Institute of Technology, under a contract with National Aeronautics Space Administration (NASA). The authors would like to thank Indrani Graczyk, JPL, for his support of the task that its results are reported in this manuscript.

REFERENCES

[1] Black, R. D., Reichert, W. M., and Turner, A. P., [Introduction for the special issue of the sensors journal: In vivo sensors for medicine] IEEE-INST ELECTRICAL ELECTRONICS ENGINEERS INC 445 HOES LANE, PISCATAWAY, NJ 08855 USA, (2008).

[2] Bocan, K. N., and Sejdić, E., "Adaptive Transcutaneous Power Transfer to Implantable Devices: A State of the Art Review," Sensors, 16(3), 393 (2016).

[3] Denisov, A., and Yeatman, E., "Ultrasonic vs. inductive power delivery for miniature biomedical implants."2010 International Conference on Body Sensor Networks, 84-89 (2010).

[4] Christensen, D. B., and Roundy, S., "Ultrasonically powered piezoelectric generators for bio-implantable sensors: Plate versus diaphragm," Journal of Intelligent Material Systems and Structures, 27(8), 1092--1105 (2016).

[5] Ozeri, S., and Shmilovitz, D., "Simultaneous backward data transmission and power harvesting in an ultrasonic transcutaneous energy transfer link employing acoustically dependent electric impedance modulation," Ultrasonics, 54(7), 1929--1937 (2014).

[6] Ozeri, S., Shmilovitz, D., Singer, S. *et al.*, "Ultrasonic transcutaneous energy transfer using a continuous wave 650kHz Gaussian shaded transmitter," Ultrasonics, 50(7), 666--674 (2010).

[7] Shahab, S., and Erturk, A., "Contactless ultrasonic energy transfer for wireless systems: acoustic-piezoelectric structure interaction modeling and performance enhancement," Smart Materials and Structures, 23(12), 1--13 (2014).

[8] Miller, D. L., "Safety assurance in obstetrical ultrasound."Seminars in Ultrasound, CT and MRI 29, 156--164 (2008).

[9] Sherrit, S., Leary, S. P., Dolgin, B. P. *et al.*, "Comparison of the Mason and KLM equivalent circuits for piezoelectric resonators in the thickness mode," Ultrasonics Symposium, 2, 921--926 vol.2 (1999).

[10] Castillo, M., "KLM model for lossy piezoelectric transducers," Ultrasonics, 41(8), 671--679 (2003).

[11] Oakley, C. G., "Calculation of ultrasonic transducer signal-to-noise ratios using the KLM model," IEEE transactions on ultrasonics, ferroelectrics, and frequency control, (1997).

[12] Van Kervel, S. J. H., "A calculation scheme for the optimum design of ultrasonic transducers," Ultrasonics, 21(3), 134-140 (1983).

[13] Moten, S., [Modeling of an ultrasonic transducer for cardiac imaging] Tech. Rep. D&C 2010.049, Dynamics and Control Group, Eindhoven University of Technology, (2010).

[14] Smith, W., "MODELING 1-3 COMPOSITE PIEZOELECTRICS - HYDROSTATIC RESPONSE," IEEE transactions on ultrasonics, ferroelectrics, and frequency control, 40(1), 41--49 (1993).